# Brillouin Frequency Shift Estimation for Brillouin Optical Time Domain Analysis Using Brillouin Gain and Loss Spectra With SVC

Hayato Nonogaki, Kazuki Hoshino, Daiki Saito, Mohd Saiful Dzulkefly Bin Zan, *Senior Member, IEEE*, and Yosuke Tanaka, *Member, IEEE*

Abstract—We propose and investigate a method to estimate Brillouin frequency shift (BFS) for Brillouin optical time domain analysis (BOTDA) using Brillouin gain and loss spectra (BGS and BLS) along with support vector machine classifier (SVC) that is one of the typical machine learning (ML) models. BGS and BLS are simultaneously swept by dual-frequency probe light, where a curve with double peaks is obtained as a function of sweep frequency. We call the obtained curve the virtual gain spectrum (VGS), from which BFS is estimated. We conducted simulation to investigate the effect of the signal-to-noise ratio (SNR) and the number of sweep points in terms of BFS estimation. Besides, the accuracy of the proposed BFS estimation method was evaluated by the experiments. Both simulation and experimental results showed that the proposed method using VGS exhibits less error in BFS estimation compared to the conventional method using BGS. In the experiment, when the frequency of probe light was swept with a step of 1 MHz, the average standard deviation of estimated BFS was 0.713 MHz in VGS SVC, while it was 1.434 MHz in BGS SVC. Even when the frequency sweep step was 10 MHz, the average standard deviation was 0.930 MHz in VGS SVC, whereas it was 3.301 MHz in BGS SVC.

Index Terms— Brillouin optical time domain analysis (BOTDA), Brillouin scattering, optical fiber sensor, support vector machine classifier (SVC).
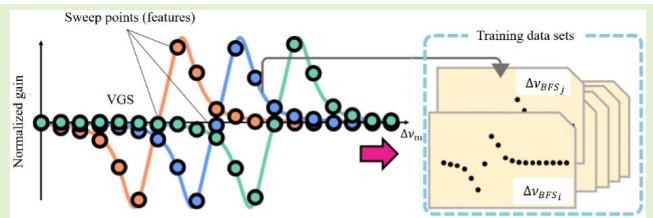
I. INTRODUCTION

DISTRIBUTED Brillouin fiber optic sensors have been intensively studied for the past decades because of their potential applications to practical use in structural health monitoring and other applications [1], [2]. They can measure temperature or strain distributed along a single optical fiber without being affected by electromagnetic noise and without requiring electrical power supply for the sensing sections. Since optical fibers are thin, flexible, and lightweight, they can be installed in a variety of structures. There are several ways to realize the distributed sensing based on Brillouin scattering. One of the typical techniques is Brillouin optical time domain analysis (BOTDA), in which pulsed pump light and continuous wave (CW) probe light are injected from the opposite ends of an optical fiber to induce stimulated Brillouin scattering (SBS) only at a position where the pump pulse exists [3]. Another technique is Brillouin optical time domain reflectometry (BOTDR), which uses spontaneous Brillouin scattering induced by optical pump pulses injected from one end of the optical fiber [4]. Brillouin optical coherence domain analysis (BOCDA) [5] and reflectometry (BOCDR) [6] have also been studied for decades as effective techniques to achieve high spatial resolution. Among these methods, BOTDA can realize relatively high optical signal-to-noise ratio (SNR) with a simple setup. In common with all the other Brillouin sensing techniques, BOTDA basically measures temperature or strain from the frequency shift of the Brillouin gain spectrum (BGS), or more precisely speaking, from the change in frequency difference between BGS and pump light, known as Brillouin frequency shift (BFS), where BFS has a linear dependence on temperature or strain of an optical fiber. In conventional BOTDA, the frequency of the probe light is scanned to monitor the BGS and measure the BFS change, where a small scanning step over a wide frequency range is required to achieve high resolution of temperature or strain measurement with a wide dynamic range. Furthermore, data averaging of up to $10\,000$ or more times is generally required to suppress the

effect of noise, which is time-consuming. Various approaches have been proposed to reduce the measurement time, such as simultaneous measurement of BGS using optical frequency comb [7], [8] and chirped probe light [9]. The slope-assisted (SA) method [10], [11], [12] is also an effective approach, which is attractive from the viewpoint of simplicity of the system setup. SA method fixes the probe frequency and measures BFS change from the probe power change based on one-to-one relationship between Brillouin gain and BFS. While SA method can reduce the measurement time, the conventional SA techniques are suffering from a restricted BFS measurement range due to limited slope area of BGS. Recently, we have proposed SA-BOTDA using multifrequency pump and probe light along with spectral shaping techniques [13], [14], [15], [16], which has expanded a linear response region up to 100 MHz of BFS. However, there is still another problem that SA-BOTDA is more susceptible to optical power fluctuation than the conventional BOTDA with frequency sweep because of the fixed probe frequency. This problem implies that Brillouin gain measurement at multiple frequencies is necessary for reducing the error. On the other hand, it is not desirable to increase the number of measurement points in the frequency domain, because it increases the measurement time. Recently, it has been found that such a tradeoff problem can be solved by introducing machine learning (ML). Among various types of ML, support vector machine (SVM), a supervised ML model applicable to classification and regression, has been successfully used in Brillouin fiber optic sensors [17], [18], [19]. Especially, SVM classifier (SVC) has been widely used for data classification. Basically, SVC can be applied to any kinds of fiber optic sensors. However, it is more desirable to give some further characteristic patterns to the optical signals, because such patterns make the signal classification and estimation much easier.

In this article, we propose and investigate a method to estimate BFS for BOTDA, which uses both Brillouin loss spectrum (BLS) and BGS along with SVC. A similar spectral shape was also achieved by using BGS and BLS in [20]. However, the system configuration in our study is further simplified by introducing serrodyne modulation for frequency shifts. The proposed technique is also similar to [14]. However, Saito and Tanaka [14] focus on realizing a linear relationship between the output signal power and BFS change. The proposed method generates a spectral shape that allows SVC to work effectively, which does not necessarily achieve a linear relationship.

II. VGS GENERATION BY BRILLOUIN GAIN AND LOSS SPECTRA

Fig. 1 illustrates the relationship between BGS, BLS, pump, and dual frequency probe in the proposed BOTDA. The profile of BGS is expressed by a Lorentzian curve with a peak at the frequency downshifted by BFS from the pump frequency and is expressed as [21]

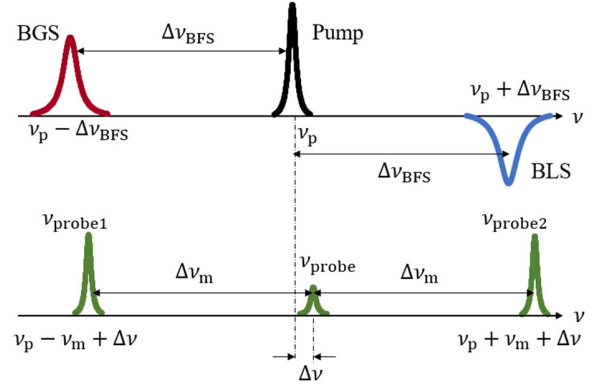$$G(v) = \frac{g_0 (\Delta v_g/2)^2}{\{v - (v_p - \Delta v_{BFS})\}^2 + (\Delta v_g/2)^2}, \quad (1)$$

Fig. 1. Relationship between BGS, BLS, pump, and dual frequency probe in the proposed BOTDA.

where Δv_g is the BGS linewidth or full-width at half-maximum (FWHM) and g_0 is the peak gain of the spectrum. BLS is generated at the frequency upshifted by Δv_{BFS} from the pump frequency and is expressed as

$$L(v) = \frac{-g_0 (\Delta v_g/2)^2}{\{v - (v_p + \Delta v_{BFS})\}^2 + (\Delta v_g/2)^2}. \quad (2)$$

In the proposed method, BGS and BLS are swept simultaneously by dual frequency probe with frequency components at

$$v_{probe1} = v_p + \Delta v - \Delta v_m \quad (3)$$

and

$$v_{probe2} = v_p + \Delta v + \Delta v_m \quad (4)$$

where

$$\Delta v = \frac{v_{probe1} + v_{probe2}}{2} - v_p. \quad (5)$$

In the measurement, the frequency spacing $2\Delta v_m$ between the two frequency components of the probe light is changed step by step, while $v_p + \Delta v$ is fixed. The total probe gain is obtained by the process that the lower frequency component of the probe light is amplified by BGS and that the higher one is attenuated by BLS. We define the total Brillouin gain as

$$A(\Delta v_{BFS}) \propto \frac{G(v_{probe1}) I_{probe1} + L(v_{probe2}) I_{probe2}}{I_{probe1} + I_{probe2}}$$

$$\propto \frac{g_0 (\Delta v_g/2)^2}{(\Delta v + \Delta v_{BFS} - \Delta v_m)^2 + (\Delta v_g/2)^2}$$

$$- \frac{g_0 (\Delta v_g/2)^2}{(\Delta v - \Delta v_{BFS} + \Delta v_m)^2 + (\Delta v_g/2)^2}, \quad (6)$$

where I_{probe1} and I_{probe2} are the intensities of probe frequency components, which satisfy $I_{probe1} = I_{probe2}$.

The proposed method changes $2\Delta v_m$ in constant steps to obtain the data required for SVC. Fig. 2 illustrates the relationship between VGS and Δv_m sweep points. VGS is composed of discrete sweep points, and BFS is labeled using this pattern in SVC. Compared to BGS with only a single peak, VGS with two peaks is speculated to enhance the accuracy
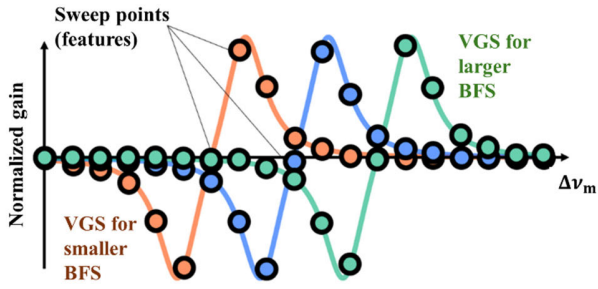
Fig. 2. Virtual gain spectrum (VGS) with different BFS changes. The VGS curve shifts to the right for larger BFS and to the left for smaller BFS.
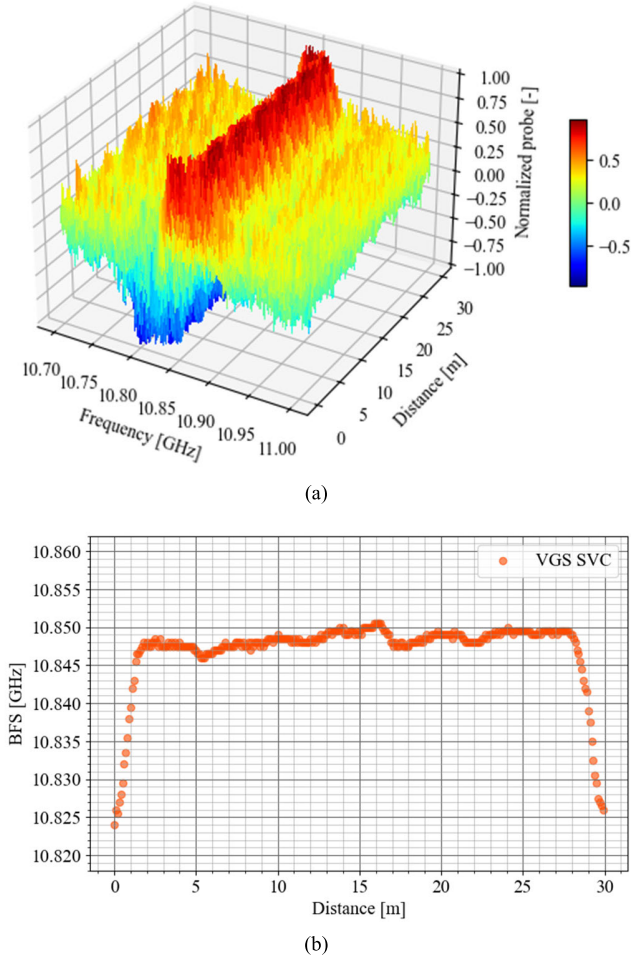

(a)

(b)

Fig. 3. Example of (a) VGS distribution measured along an optical fiber and (b) BFS distribution derived by applying SVC.
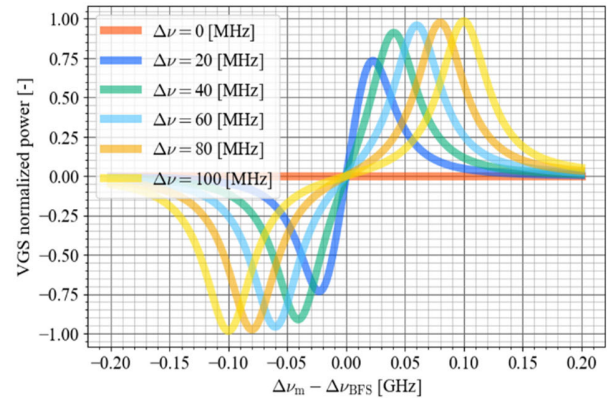

Fig. 4. Normalized VGS for $\Delta\nu$ of 0, 20, 40, 60, 80, and 100 MHz with a BGS bandwidth $\Delta\nu_g$ of 50 MHz.

increase the error in BFS estimation, even when the probe frequency scanning step is coarse.

III. SIMULATION ON BFS ESTIMATION WITH VGS AND SVC

The error of BFS estimation in the proposed method using VGS was investigated by simulation varying the SNR of BGS and $\Delta\nu$. Fig. 4 shows the normalized VGS with different $\Delta\nu$ values, where the peak gain of BGS is one. In this simulation, we defined SNR of BGS as the ratio of the gain peak to the noise amplitude. In addition, the SNRs of BGS and BLS are assumed to be the same. The noise is assumed to be randomly generated white noise. Table I shows the parameters of the training data for the SVC model. The SVC model was trained with 12 261 data ($N_{\text{class}} \times N_{\text{FWHMs}} = N_{\text{train}}$) of VGS generated by different BGS and BLS composed of pure Lorentzian curves with different FWHMs of 20–80 MHz. N_{class} is the number of classes with 201 types, categorizing 10.780–10.880-GHz frequency range in 0.5-MHz steps. N_{FWHMs} is the number of FWHM types, and there are 61 types of FWHMs, categorized by 1 MHz from 20 to 80 MHz. After the training, the SVC model was evaluated by the test dataset created under almost the same conditions except that the noise was added to the data. The training and test data were generated by a computer based on (6).

Table II shows the parameters of the test data for the SVC model. First, we set $\Delta\nu$ at 20 MHz. We supposed that the frequency $\Delta\nu_m$ was scanned from 10.7 to 11.0 GHz, which covers the entire VGS spectrum. We evaluated the accuracy of BFS estimation at different scanning steps by simulation. The frequency scanning step was 1, 2, 5, or 10 MHz.

Fig. 5 shows the root mean square error (RMSE) of the estimation results from the set BFS. Fig. 5 also shows the RMSE of the estimation results based on curve fitting of the entire VGS data for comparison.

As the sweep frequency step $\Delta\nu_{m\_\text{step}}$ becomes coarser, the RMSE becomes larger, which indicates that the BFS estimation accuracy gets worse. For example, when $\Delta\nu_{m\_\text{step}}$ is 1 MHz [Fig. 5(a)], the RMSE is less than 5 MHz, whereas when $\Delta\nu_{m\_\text{step}}$ is 10 MHz [Fig. 5(d)], the RMSE can be up to 20 MHz or more. However, there is not much difference between BFS estimation by Lorentzian curve fitting (LCF) and

of BFS estimation by SVC due to its distinctive gain shape pattern and the broader frequency range it covers.

In BOTDA, we first measure the VGS distribution along an optical fiber. Fig. 3(a) shows an example of a real VGS distribution. The BFS at each position is derived by applying the SVC to the VGS at that position. Here, the SVC has been pretrained by a large amount of computer-generated pattern matching data relating VGS to BFS. Finally, the SVC derives the BFS distribution from the VGS. Fig. 3(b) shows an example of the derived BFS distribution. As will be shown in Sections III and IV, the proposed method does not significantly
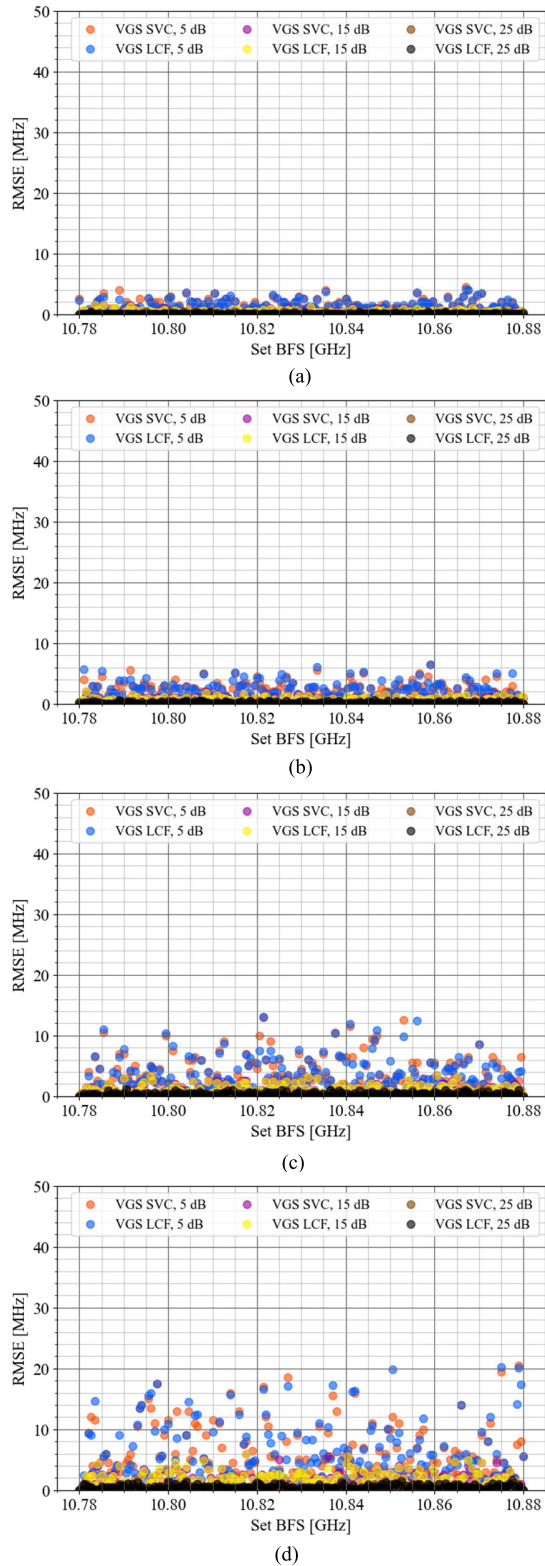
(a)

(b)

(c)

(d)

Fig. 5.   Relationship between RMSE of estimated BFS and set BFS in VGS SVC and VGS LCF, where $\Delta\nu$ is 20 MHz and $\Delta\nu_{m\_step}$ is (a) 1, (b) 2, (c) 5, and (d) 10 MHz.

(a)

(b)

(c)

(d)

Fig. 6.   Relationship between RMSE of estimated BFS and set BFS in BGS SVC and BGS LCF, where $\Delta\nu_{m\_step}$ is (a) 1, (b) 2, (c) 5, and (d) 10 MHz.

BFS estimation by SVC. We speculate that this is because the SVC model assumes a pure Lorentzian curve without noise based on mathematical equations, and the BFS estimation with SVC may have worked similar to curve fitting.
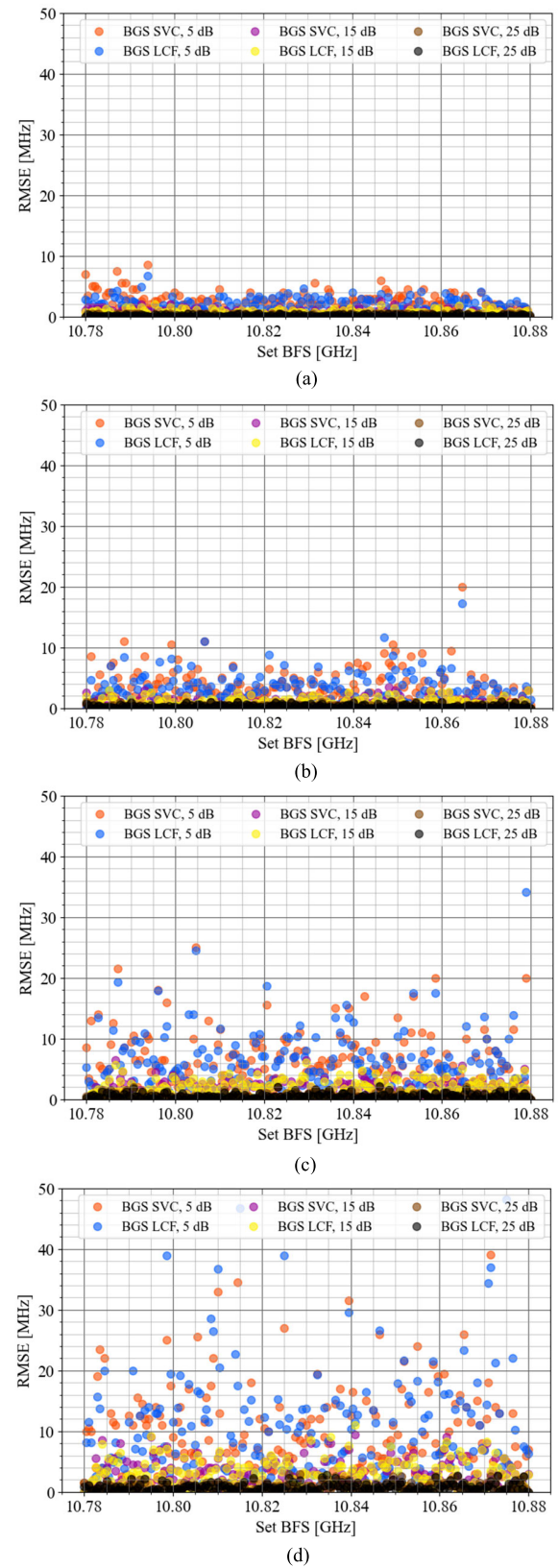
We also investigated by simulation the dependence of BFS estimation accuracy on the sweep step in the case of BGS in Fig. 6. The RMSE of BGS becomes larger for the coarser

TABLE I
PARAMETERS OF TRAINING DATASETS FOR THE SIMULATION OF BFS
ESTIMATION AT DIFFERENT SCANNING STEPS BY SIMULATION

Symbol	Description	Value
$\Delta\nu$	Center frequency difference [MHz]	20
$\Delta\nu_{\text{BFS\_train}}$	Learning BFS [GHz]	10.780 - 10.880
$\Delta\nu_{\text{BFS\_trainstep}}$	Learning BFS step [MHz]	0.5
N_{class}	Number of classifications	201
$\Delta\nu_{\text{g\_train}}$	Learning half-width [MHz]	20 - 80
$\Delta\nu_{\text{g\_trainstep}}$	Learning half-width step [MHz]	1
N_{FWHMs}	Number of FWHMs	61
N_{train}	Number of training data ($N_{\text{class}} \times N_{\text{FWHMs}}$)	12,261

TABLE II
PARAMETERS OF TEST DATASETS FOR THE SIMULATION OF BFS
ESTIMATION AT DIFFERENT SCANNING STEPS BY SIMULATION

Symbol	Description	Value
$\Delta\nu$	Center frequency difference [MHz]	20
$\Delta\nu_{\text{BFS\_test}}$	BFS range [GHz]	10.780 - 10.880
$\Delta\nu_{\text{BFS\_teststep}}$	BFS step [MHz]	0.5
N_{class}	Number of classifications	201
$\Delta\nu_{\text{m}}$	Sweep range [GHz]	10.700 - 11.000
$\Delta\nu_{\text{m\_step}}$	Sweep step [MHz]	1, 2, 5, or 10
$N_{\Delta\nu\text{m\_step}}$	Number of $\Delta\nu_{\text{m}}$ step	4
$\Delta\nu_{\text{g\_test}}$	Half-width [MHz]	50
N_{FWHMs}	Number of FWHMs	1
-	SNR [dB]	5 - 50
-	SNR step [dB]	10
N_{SNR}	Number of SNR	5
N_{test}	Number of test data ($N_{\text{class}} \times N_{\text{FWHMs}} \times N_{\text{SNR}}$ per each $\Delta\nu_{\text{m}}$ step)	2010 (per each $\Delta\nu_{\text{m}}$ step)

sweep step. Comparing under the same sweep range, the deterioration of RMSE is larger in BGS than in VGS. The RMSE in VGS is lower because VGS has a wider nonzero spectral range than BGS, which makes the amount of information contributing to SVC relatively larger when the sweep step is coarser. To further discuss the simulation results in Figs. 5 and 6, we calculated the average value in the RMSE from set BFS which ranged from 10.780 to 10.880. We then compared BFS estimation accuracy per SNR for each method in Fig. 7. As previously observed, VGS has higher BFS estimation accuracy than BGS for both LCF and SVC at low SNR. Additionally, the coarser sweep step results in lower BFS estimation accuracy. No significant differences were observed for LCF and SVC.

Fig. 8 shows the RMSE of BFS estimation as a function of $\Delta\nu$ for different SNRs. The results are also compared with each method at different sweep steps, as shown in Fig. 7. This simulation was used to determine the optimal $\Delta\nu$ for the experiments in Section IV. The parameters for both training and test data were the same as in Tables I and II, except for $\Delta\nu$ (as shown in Tables III and IV).

In Fig. 8(a)–(d), the error in BFS estimation is large for the case of $\Delta\nu$ of less than 20 MHz. This can be explained from the fact that the decrease in $\Delta\nu$ makes the amplitude of VGS smaller (Fig. 3) and less informative both for the
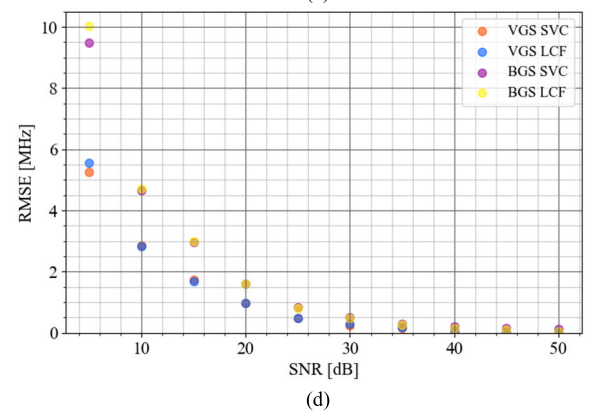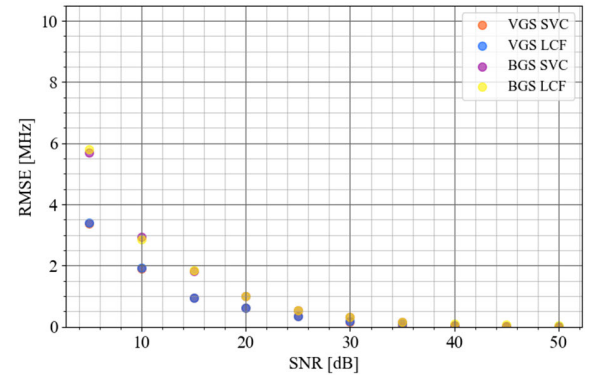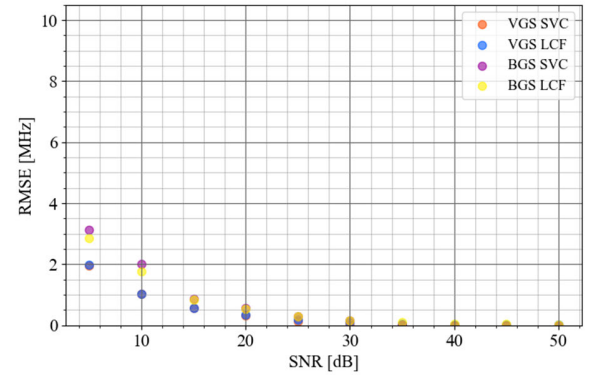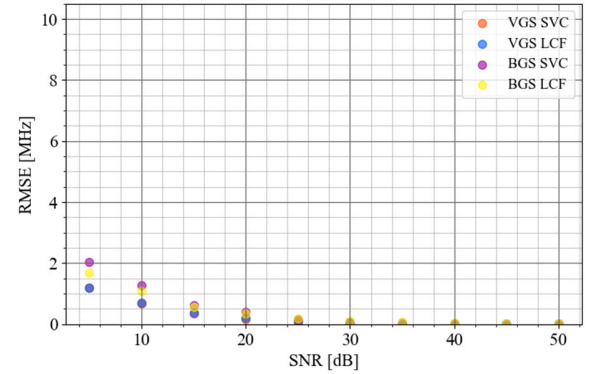

Fig. 7. RMSE of BFS estimation as a function of SNR for $\Delta\nu$ of 20 MHz and $\Delta\nu_{\text{m\_step}}$ of (a) 1, (b) 2, (c) 5, and (d) 10 MHz.

curve fitting and the proposed methods. Furthermore, setting $\Delta\nu$ to around 80 MHz or higher also results in an increase in RMSE. Based on these results, we set $\Delta\nu$ at 20 MHz in the experiments that will be shown in Section IV.
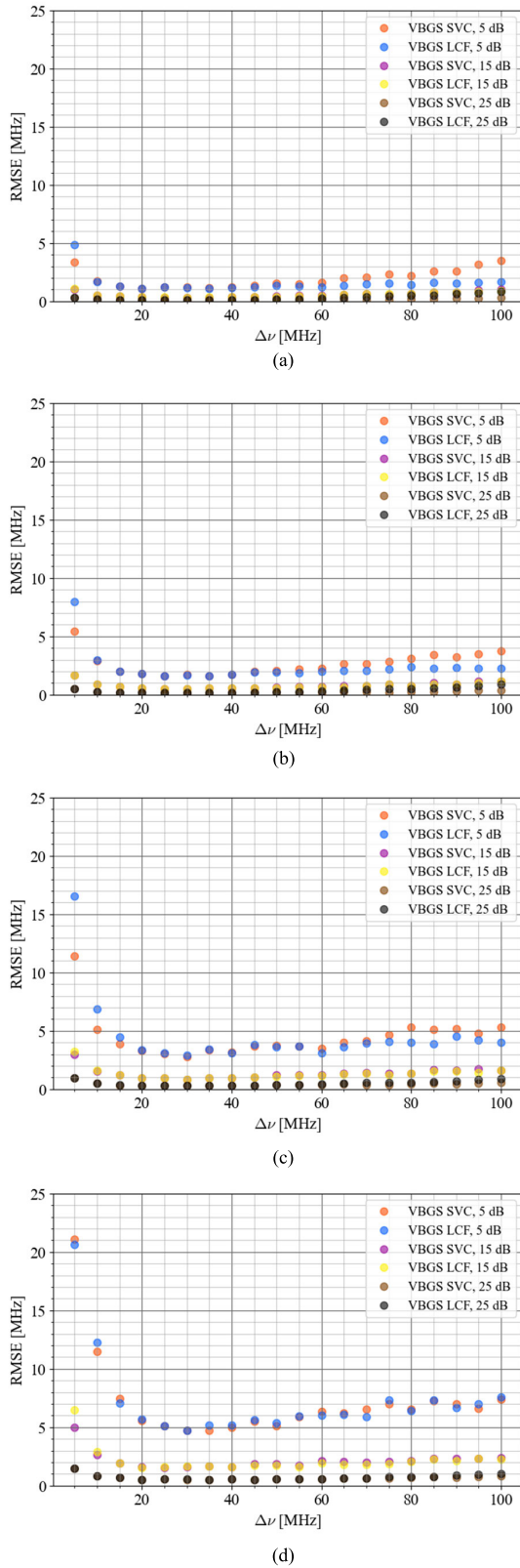
Fig. 8. RMSE of BFS estimation as a function is $\Delta\nu$, where $\Delta\nu_{m\_step}$ is (a) 1, (b) 2, (c) 5, and (d) 10 MHz.

TABLE III
PARAMETERS OF TRAINING DATASETS FOR THE SIMULATION OF BFS ESTIMATION AT DIFFERENT $\Delta\nu$ VALUES

Symbol	Description	Value
$\Delta\nu$	Center frequency difference [MHz]	5 - 100
$\Delta\nu_{step}$	Frequency shift step for $\Delta\nu$ [MHz]	5
$N_{\Delta\nu\_step}$	Number of frequency shift steps for $\Delta\nu$	20
$\Delta\nu_{BFS\_train}$	Learning BFS [GHz]	10.780 - 10.880
$\Delta\nu_{BFS\_trainstep}$	Learning BFS step [MHz]	0.5
N_{class}	Number of classifications	201
$\Delta\nu_{g\_train}$	Learning half-width [MHz]	20 - 80
$\Delta\nu_{g\_trainstep}$	Learning half-width step [MHz]	1
N_{FWHMs}	Number of FWHMs	61
N_{train}	Number of training data ($N_{class} \times$ N_{FWHMs} per each $\Delta\nu$)	12261 (per each $\Delta\nu$)

TABLE IV
PARAMETERS OF TEST DATASETS FOR THE SIMULATION OF BFS ESTIMATION AT DIFFERENT $\Delta\nu$ VALUES

Symbol	Description	Value
$\Delta\nu$	Center frequency difference [MHz]	5 - 100
$\Delta\nu_{step}$	Frequency shift step for $\Delta\nu$ [MHz]	5
$N_{\Delta\nu\_step}$	Number of frequency shift steps for $\Delta\nu$	20
$\Delta\nu_{BFS\_test}$	BFS range [GHz]	10.780 - 10.880
$\Delta\nu_{BFS\_teststep}$	BFS step [MHz]	0.5
N_{class}	Number of classifications	201
$\Delta\nu_{m}$	Sweep range [GHz]	10.700 - 11.000
$\Delta\nu_{m\_step}$	Sweep step [MHz]	1, 2, 5, or 10
$\Delta\nu_{g\_test}$	Half-width [MHz]	50
N_{FWHMs}	Number of FWHMs	1
-	SNR [dB]	5 – 50
-	SNR step [dB]	5
N_{SNR}	Number of SNR	10
N_{test}	Number of test data ($N_{class} \times N_{FWHMs} \times$ N_{SNR} per each $\Delta\nu$)	2010 (per each $\Delta\nu$)

deviation of the BFS obtained from the distributed measurements along the FUT. As this experiment aimed to confirm the simulation results in Section III, the learning model used was identical to that in Table I, generated by a computer based on (6).

Fig. 9 shows the experimental setup. The laser beam with a wavelength of 1.55 μm from a laser diode (LD) was split by a 3-dB coupler. One beam was used as a pump light and the other as a probe light. In the pump arm, the light was modulated with pulses at the repetition rate of 2.5 MHz by an intensity modulator (IM1). The pulsewidth was set to 25 ns, which corresponds to a spatial resolution of 2.5 m. The pump pulse was amplified by an EDFA and then injected into a fiber under test (FUT). In the probe arm, a saw-wave modulation called serrodyne modulation was applied to the light by a phase modulator (PM), which shifted the optical frequency by $\Delta\nu$. Then, the light was deeply modulated with a frequency $\Delta\nu_m$ by an intensity modulator (IM2) to generate sidebands

IV. EXPERIMENTAL EVALUATION OF BFS ESTIMATION ACCURACY OF DISTRIBUTED FIBER OPTIC SENSING USING VGS WITH SVC

In this section, the accuracy of BFS estimation by the proposed method is evaluated by calculating the standard
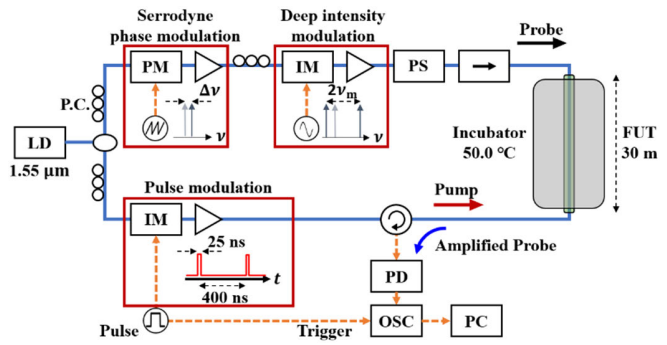
Fig. 9. Experimental setup for fiber optic sensing using Brillouin loss and gain spectra. LD: laser diode. PM: phase modulator. IM: intensity modulator. PS: polarization scrambler. FUT: fiber under test. PD: photodiode. OSC: oscilloscope. PC: personal computer.

without a carrier component. The modulation frequency was 10.700–11.000 GHz that covered the entire VGS. The probe light passed through a polarization scrambler (PS), before injected into the FUT, where the one frequency component was amplified by BGS and the other was attenuated by BLS. The optical signal detected by a photodiode (PD) was averaged over 5000 times and monitored by an oscilloscope (OSC). The FUT was a 30-m-long single-mode fiber, where the whole fiber length was set in an incubator. The temperature inside the incubator was set to 50.0 °C. Measurement data for 30 m were obtained in 0.1 m increments by acquiring 300 points with an oscilloscope at 1 GSa/s. An experiment of BOTDA using BGS was also conducted for comparison with a similar setup except that PM was not used and the upper frequency component after IM was cut by a filter in the probe branch. We only compared the accuracy of BFS measurements, which depends on the difference between VGS and BGS gain types. We kept other conditions, such as pump power, the same as much as possible in the BFS measurement. SNR was also standardized to a constant value to ensure the equivalent conditions.

The BFS distribution was derived from the VGS distribution obtained by setting $\Delta\nu_{m\_step}$ to 1, 2, 5, or 10 MHz in the same way as in the simulations. Since the temperature in the incubator was kept constant, the BFS was expected to have a constant value along FUT except for the effect of pretension and a spatial distribution of temperature within 1 °C in the incubator. Fig. 10 shows the estimated BFS distributions for different sweep steps.

The coarser sweep step made the variation in BFS larger in all the cases. However, the variation was larger in BGS SVC than in VGS SVC. Significant difference was not observed in LCF for both VGS and BGS. These were consistent with the simulation results and their interpretation in Section III.

The same experiments were conducted five times for each condition, and the standard deviation of the BFS for each distance was calculated (Fig. 11). The average standard deviation was calculated at distances from 5 to 25 m from the starting point of the FUT as a function of sweep step (Fig. 12). As the sweep step becomes coarser from 1 to 10 MHz, the average standard deviation in VGS SVC changed from 0.713 to 0.930 MHz, which is an increase by 30.4%, whereas
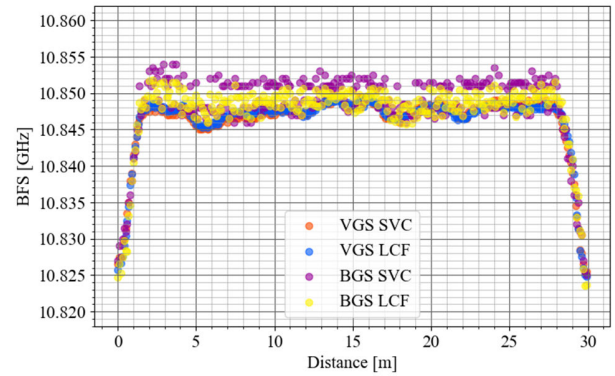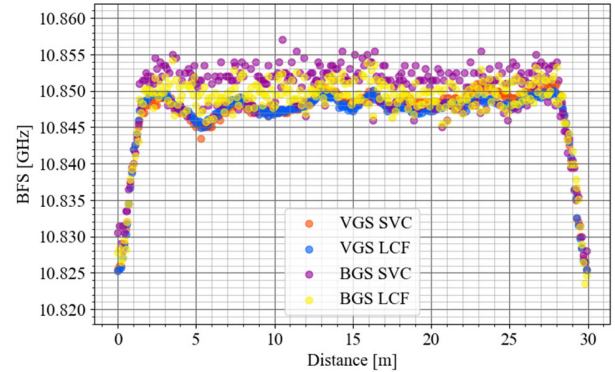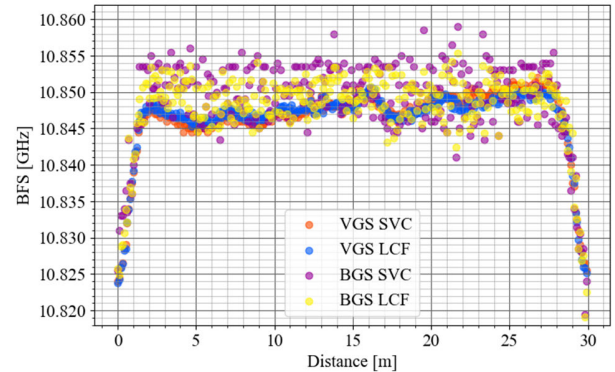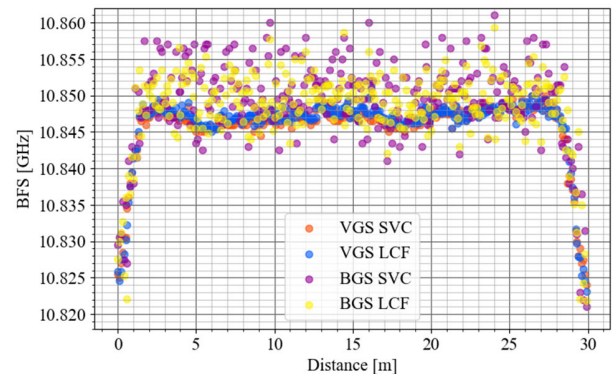

Fig. 10. Estimated BFS obtained by distributed measurement, where $\Delta\nu_{m\_step}$ is (a) 1, (b) 2, (c) 5, and (d) 10 MHz.

it changed from 1.454 to 3.301 MHz in BGS SVC, which is an increase by 127%. The accuracy of BFS estimation by
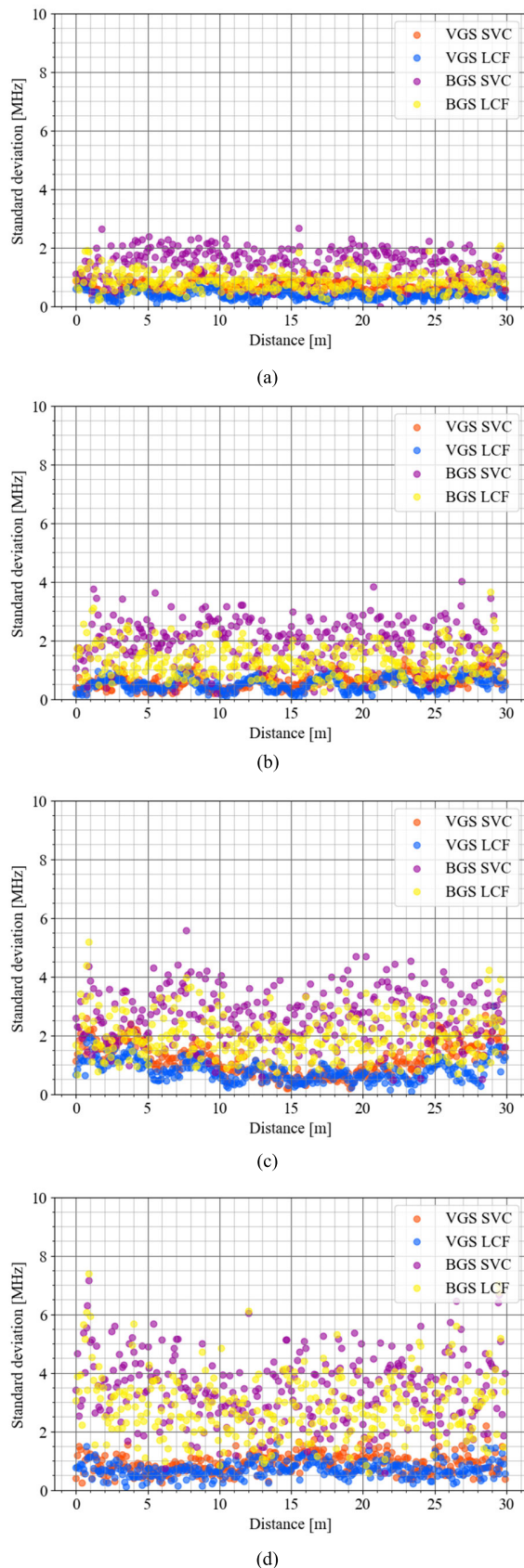
(a)

(b)

(c)

(d)

Fig. 11.   Standard deviations of estimated BFS obtained by distributed measurement, where $\Delta\nu_{m\_step}$ is (a) 1, (b) 2, (c) 5, and (d) 10 MHz.

VGS LCF and VGS SVC was found to be almost equal, which agrees with the simulation results.
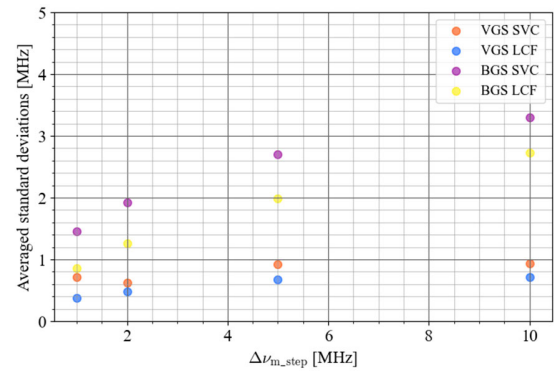

Fig. 12.   Average standard deviation calculated at distances from 5 to 25 m from the starting point of the FUT.

V. CONCLUSION

We have proposed a method to estimate BFS in BOTDA by using VGS, which is a virtually synthesized spectrum based on BGS and BLS, with the help of SVC. Simulations and experiments have confirmed that the proposed method based on VGS has less degradation in BFS estimation accuracy due to coarse sweep step of probe light frequency compared with conventional BOTDA using BGS. On the other hand, there was no significant difference in the standard deviation between the VGS LCF and the VGS SVC. This may be because we used pure Lorentzian curve both for curve fitting and for generating training data for SVC. A major difference between them is the prospect that SVC can estimate BFS without using mathematical expressions, such as Lorentzian, Voigt, and others for VGS. A large amount of experimentally obtained data of VGS and BFS can also be related and classified by SVC, which is a next step of this study.

REFERENCES

[1] H.-N. Li, D.-S. Li, and G.-B. Song, "Recent applications of fiber optic sensors to health monitoring in civil engineering," *Eng. Struct.*, vol. 26, no. 11, pp. 1647–1657, Sep. 2004.

[2] X. Bao and L. Chen, "Recent progress in Brillouin scattering based fiber sensors," *Sensors*, vol. 11, no. 4, pp. 4152–4187, Apr. 2011.

[3] T. Horiguchi and M. Tateda, "BOTDA-nondestructive measurement of single-mode optical fiber attenuation characteristics using Brillouin interaction: Theory," *J. Lightw. Technol.*, vol. 7, no. 8, pp. 1170–1176, Aug. 1989.

[4] T. Horiguchi, K. Shimizu, T. Kurashima, M. Tateda, and Y. Koyamada, "Development of a distributed sensing technique using Brillouin scattering," *J. Lightw. Technol.*, vol. 13, no. 7, pp. 1296–1302, Jul. 13, 1995.

[5] K. Hotate and T. Hasegawa, "Measurement of Brillouin gain spectrum distribution along an optical fiber using a correlation-based technique—Proposal, experiment and simulation," *IEICE Trans. Electron.*, vols. E83–C, no. 3, pp. 405–412, Mar. 2000.

[6] Y. Mizuno, Z. He, and K. Hotate, "One-end-access high-speed distributed strain measurement with 13-mm spatial resolution based on Brillouin optical correlation-domain reflectometry," *IEEE Photon. Technol. Lett.*, vol. 21, no. 7, pp. 474–476, Feb. 3, 2009.

[7] C. Jin et al., "Scanning-free BOTDA based on ultra-fine digital optical frequency comb," *Opt. Exp.*, vol. 23, no. 4, p. 5277, Feb. 2015.

[8] Y. Tanaka and Y. Ozaki, "Brillouin frequency shift measurement with virtually controlled sensitivity," *Appl. Phys. Exp.*, vol. 10, no. 6, Jun. 2017, Art. no. 062504.

[9] D. Zhou et al., "Single-shot BOTDA based on an optical chirp chain probe wave for distributed ultrafast measurement," *Light, Sci. Appl.*, vol. 7, no. 1, p. 32, Jul. 2018.

[10] Y. Peled, A. Motil, L. Yaron, and M. Tur, "Slope-assisted fast distributed sensing in optical fibers with arbitrary Brillouin profile," *Opt. Exp.*, vol. 19, no. 21, p. 19845, Oct. 2011.

[11] H. Lee, N. Hayashi, Y. Mizuno, and K. Nakamura, "Slope-assisted Brillouin optical correlation-domain reflectometry: Proof of concept," *IEEE Photon. J.*, vol. 8, no. 3, pp. 1–7, Jun. 2016.

[12] D. Zhou et al., "Slope-assisted BOTDA based on vector SBS and frequency-agile technique for wide-strain-range dynamic measurements," *Opt. Exp.*, vol. 25, no. 3, pp. 1889–1902, 2017.

[13] Y. Tanaka and T. Hasegawa, "Brillouin optical time domain analysis using spectrally reshaped 12-GHz spacing multimode pump and probe," in *Proc. Conf. Lasers Electro-Optics (CLEO)*, vol. 7, May 2020, pp. 1–2.

[14] D. Saito and Y. Tanaka, "Slope assisted Brillouin optical time domain analysis using dual frequency probe with gain and loss spectra," in *Proc. Conf. Lasers Electro-Optics (CLEO)*, May 2021, pp. 1–2.

[15] K. Hoshino, D. Saito, M. S. Dz. Zan, and Y. Tanaka, "Distributed strain sensing using slope assisted BOTDA based on virtual Brillouin gain spectrum synthesized by multi-frequency light," *Proc. SPIE*, vol. 11914, Nov. 2021, Art. no. 1191409.

[16] K. Hoshino, D. Saito, Y. Endo, T. Hasegawa, and Y. Tanaka, "Brillouin gain spectrum manipulation using multifrequency pump and probe for slope-assisted BOTDA with wider dynamic range," *Appl. Phys. Exp.*, vol. 15, no. 2, Feb. 2022, Art. no. 022009.

[17] H. Wu, L. Wang, N. Guo, C. Shu, and C. Lu, "Brillouin optical time-domain analyzer assisted by support vector machine for ultra-fast temperature extraction," *J. Lightw. Technol.*, vol. 35, no. 19, pp. 4159–4167, Aug. 14, 2017.

[18] H. Zhu et al., "Optimized support vector machine assisted BOTDA for temperature extraction with accuracy enhancement," *IEEE Photon. J.*, vol. 12, no. 1, pp. 1–14, Feb. 2020.

[19] O. Furukawa, "A study on thermal detection based on support vector machine using dynamic time warping and application to optical fiber sensor," *IEEE Sensors J.*, vol. 21, no. 5, pp. 6325–6334, Mar. 2021.

[20] C. Feng, X. Lu, S. Preussler, and T. Schneider, "Gain spectrum engineering in distributed Brillouin fiber sensors," *J. Lightw. Technol.*, vol. 37, no. 20, pp. 5231–5237, Oct. 15, 2019.

[21] A. Kobyakov, M. Sauer, and D. Chowdhury, "Stimulated Brillouin scattering in optical fibers," *Adv. Opt. Photon.*, vol. 2, no. 1, pp. 1–59, Mar. 2010.
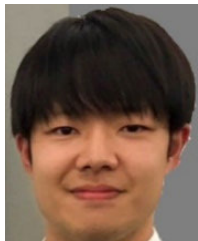
Hayato Nonogaki received the B.E. degree in electrical and electronic engineering from Tokyo University of Agriculture and Technology (TUAT), Tokyo, Japan, in 2022, where he is currently pursuing the M.E. degree.

His current interests include distributed Brillouin fiber optic sensors.

Kazuki Hoshino, photograph and biography not available at the time of publication.

Daiki Saito, photograph and biography not available at the time of publication.

Mohd Saiful Dzulkefly Bin Zan (Senior Member, IEEE) received the B.E. degree in electronics, information, and communication engineering from Waseda University, Tokyo, Japan, in 2006, and the M.Eng. and Dr.Eng. degrees from Shibaura Institute of Technology, Tokyo, in 2011 and 2014, respectively.

He was a Postdoctoral Researcher at Shibaura Institute of Technology from 2017 to 2018. He is currently an Associate Professor with Universiti Kebangsaan Malaysia, Bangi, Malaysia. His research interests include centered around the distributed optical fiber sensors (DOFS), such as Brillouin-based DOFS and Rayleigh-based DOFS. Apart from that, he is also conducting research on fiber Bragg grating (FBG) sensors.

Dr. Zan is a Senior Member of OPTICA.

Yosuke Tanaka (Member, IEEE) received the B.E. degree in electronic engineering and the M.E. and Dr.Eng. degrees in electrical engineering from the University of Tokyo, Tokyo, Japan, in 1991, 1993, and 1996, respectively.

After working at Shizuoka University, Shizuoka, Japan, as a Research Associate, he joined Tokyo University of Agriculture and Technology, Tokyo, in 1999, where he is currently a Professor. His research interests include the fiber optic sensing and its related subjects, including laser-based precision measurement, high speed optical signal processing, application of optical frequency comb, and fiber optic power supply.

Dr. Tanaka is a member of the Institute of Electrical and Electronics Engineers (IEEE), OPTICA, the International Society for Optics and Photonics (SPIE), the Institute of Electronics, Information, and Communication Engineers (IEICE), and the Japan Society of Applied Physics (JSAP).